

## Photopatterning DNA Structures with Topological Defects and Arbitrary Patterns Through Multiple Length Scales

Netra Prasad Dhakal<sup>1</sup>, Jinghua Jiang,<sup>1</sup> Yubing Guo,<sup>2</sup> and Chenhui Peng<sup>1,\*</sup>

<sup>1</sup>*Department of Physics and Materials Science, The University of Memphis, Memphis, Tennessee 38152, USA*

<sup>2</sup>*Advanced Materials and Liquid Crystal Institute, Kent State University, Kent, Ohio 44242, USA*

(Received 12 September 2019; revised manuscript received 15 November 2019; published 15 January 2020)

DNA is the building block for most living organisms; hence, controlling the supramolecular self-assembly of DNA structures is important not only for a better understanding of its biological properties, but also for shedding light on the design of functional materials for biological engineering and materials science applications. However, it is still challenging to control DNA molecular self-assembly structures in a predesigned manner across multiple length scales. Here, we demonstrate that the orientational order of DNA molecules can be precisely controlled by using the photopatterning technique. This technique imprints various spatially varying patterns into a layer of liquid-crystalline polymer, which will be further used to control the DNA structures. It is demonstrated that DNA orientations can be patterned with a two-dimensional lattice of topological defects and arbitrary patterns through length scales from micrometers to millimeters. The resulting programmable and predesigned DNA self-assembly structures will open up opportunities in advanced materials and devices for optical and biological applications.

DOI: 10.1103/PhysRevApplied.13.014026

### I. INTRODUCTION

Nature has the fascinating capability to precisely control molecular building blocks, such as DNA, to assemble complex structures on multiple length scales [1]. After the double-helix structure of DNA was discovered by Watson and Crick in 1953 [2], scientists have tried to understand the DNA self-assembly properties of human beings and apply nature's approaches to design and control hierarchical assembly structures [3–7]. As a consequence, macroscopic organization and its coupled functionality show potential applications ranging from biosensing devices [8] to tissue engineering [9] and inorganic solid-state and opto-electronic devices [10–12]. Despite the advantages that well-ordered DNA assembly structures can offer, the challenge is to develop robust approaches to control the spatial organization of these assemblies across multiple length scales [3–7]. Several methods are proposed to create large-scale, well-ordered, and oriented DNA structures by using evaporation [13,14], magnetic fields [15], mechanical shearing [16], molecular combing [17–20], and topographic control [21–23]. However, these approaches control only the local domains instead of larger structures. Control of DNA molecular self-assembled structures with predetermined architecture and functionality through multiple length scales is highly desirable and

is one of the major goals of biological engineering and materials science.

The ordering structures of DNA molecules can be based on its liquid-crystal phase with spontaneous orientational order. If the concentration of an aqueous DNA solution reaches about 50 mg/mL, DNA molecules will self-assemble into a nematic phase [24]. If the concentration is high enough, up to 200 mg/mL, the DNA solution will display a columnar phase [25]. The nematic ordering of DNA structures can be controlled by using the surface-patterning technique. Here, we propose to control DNA molecular self-assembled structures by using the photopatterning technique [26]. In this approach, a plasmonic metmask is used to control the local state of light polarization, rather than via standard photomasks that control only the intensity of transmitted light, and thus, multiple exposures are eliminated [26,27]. The light beam transmitted through the plasmonic metmask acquires a spatial distribution of polarization that is imprinted onto a layer of liquid-crystalline polymer [28,29].

When an aqueous DNA solution of nematic phase contacts with the ordered and oriented polymer thin film, the DNA assembly structures can be aligned to follow the predesigned liquid-crystalline polymer orientations. This technique allows one to create any pattern of assembled ordered DNA structures, with the typical scale ranging from micrometers to millimeters. Here, we demonstrate that complex patterns of DNA molecular self-assembled structures with two-dimensional (2D) lattice of topological

\*cpeng@memphis.edu

defects are created. Patterns of DNA hierarchical structures with arbitrary geometries across multiple length scales are also achieved. The resulting programmable and predesigned DNA self-assembly structures will open up opportunities for designing biomaterials [30,31] and developing advanced functional nanomaterials [32–34] for electro-optical and biosensing applications.

## II. EXPERIMENTAL RESULTS

### A. Materials and photo-patterning

We follow the recently proposed approach for surface photoalignment that is based on plasmonic photomasks used to irradiate bounding plates with light of a controlled polarization pattern, as described in detail in Refs. [26,35]. The photosensitive material used here is an azo dye, SD1 [Fig. 1(b)], from DIC, Inc. It is mixed with *N,N*-dimethylformamide (from Sigma, Inc.) at a concentration

of 0.2 wt % and spin-coated onto the cleaned glass substrates at 3000 rpm for 30 s. After baking at 120 °C for 15 min, the SD1-coated substrates are exposed in the photopatterning setup shown in Fig. 1(f) for 5 min [36–38]. In the photopatterning setup, we use an X-Cite 120 metal halide lamp as a source of nonpolarized light to illuminate the plasmonic metamasks; the lamp output is the strongest in the spectral range between 350 and 450 nm. The plasmonic photomask is made of a quartz substrate coated with aluminum films of 150 nm thick [26]. The aluminum film is perforated by means of electron beam lithography and reactive ion etching with rectangular nanoapertures, each of 220 nm in length and 100 nm wide. An unpolarized light beam goes through the photomask and becomes linearly polarized, and the polarization is perpendicular to the long side of the nanoaperture. By designing the orientations of the nanoapertures in space, the light polarization can also be manipulated to vary from point to point [39]. Patterns with spatially varying linear polarizations are projected and imprinted on the azo-dye SD1 layer [26,35].

Due to the soluble property of the azo dye in the aqueous environment, a passivation layer of liquid-crystalline polymer covers the SD1 layer to preserve this pattern [28]. Liquid-crystalline monomer of reactive mesogen RM257 (from Wilshire, Inc.), Fig. 1(a), and photoinitiator Irgacure 651 (from Ciba) are mixed with toluene at concentrations of 7 and 0.07 wt %, respectively. This monomer solution is spin-coated onto the patterned SD1 layer at 3000 rpm for 30 s. The monomer is photopolymerized by an unpolarized UV light (UVL-26 Handheld UV lamp, Analytikjena LLC), with an intensity of 1.4 mW/cm<sup>2</sup>, wavelength 365 nm, for 30 min. The polymer pattern replicates the alignment pattern of azo dye beneath it through the interaction of RM257 molecules with the orientationally ordered chemical groups on the azo-dye layer [28]. The predesigned patterns on the SD1 layer will be transmitted to this liquid-crystalline polymer layer, which will be used to pattern orientational order of the nematic DNA solution.

Sodium salt of DNA from salmon testes (from Sigma Inc.) with 2000 base pairs [40] is used in this work. This DNA is considered to be a semiflexible polymer with a persistence length of 50 nm [41] and a nematic liquid-crystal phase will form at concentrations from 50 to 200 mg/ml [24]. DNA in the nematic phase with a concentration of 100 mg/ml is used, which has an isotropic phase at 95 °C, Fig. 1(c), and an isotropic-nematic phase transition at 90 °C, Fig. 1(d). All experiments are conducted at 25 °C in the nematic phase, Fig. 1(e).

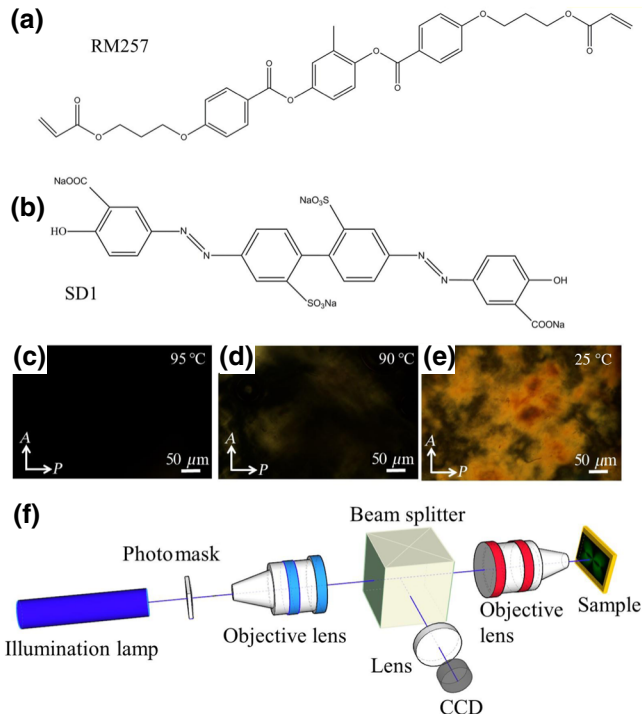


FIG. 1. Photopatterning materials and setup. (a) Molecular structure of liquid-crystalline monomer reactive mesogen RM257. (b) Molecular structure of photosensitive azo-dye SD1. Polarizing optical microscope images of DNA solution in isotropic phase at 95 °C (c), isotropic-nematic phase transition at 90 °C (d), and nematic phase at 25 °C (e). (f) Schematic of photopatterning setup. The light is emitted from the illumination lamp and patterns of linearly polarized light distribution are created after the plasmonic photomask, which are projected on the sample coated with azo-dye SD1 through two objective lens. The predesigned patterns will be imprinted onto the SD1 layer. *P* and *A* represent polarizer and analyzer, respectively.

### B. Planar alignment of DNA structures

Aqueous DNA solution with a concentration of 100 mg/ml is prepared and one drop of this solution is placed on one patterned substrate with an aligned

liquid-crystalline polymer layer. The other cleaned glass substrate will cover this DNA drop. The gap between the two substrates are set by 5- $\mu\text{m}$  glass spacers. This sample is promptly sealed by 5 min epoxy glue to avoid water evaporation. Then the sample is heated up to 95 °C to remove all flow alignment and other undesirable effects. After the sample is cooled to room temperature, the sample is imaged by using a polarizing optical microscope (POM). We use a 50X-1000X advanced upright polarized light microscope from Amscope with both 10 $\times$  Plan, NA = 0.25 objective, and 20 $\times$  Plan, NA = 0.40 objective, lenses. Optical microscopic images are captured by using a 20MP USB3.0 BSI C-mount microscope camera from Amscope (resolution 5440  $\times$  3648 pixels).

Figure 2 shows that after the nematic DNA solution contacts the liquid-crystalline polymer layer with a planar alignment, DNA chains will be aligned uniformly following this planar fasion. The alignment of DNA structures can be directly determined by using POM with a retardation  $\lambda$  plate [16,23,42]. The  $\lambda$  plate has a slow axis along 45° and alignment of DNA parallel to this axis will show yellowish domains, Figs. 2(a) and 2(b), and perpendicular to this axis will show blueish domains, Figs. 2(c) and 2(d).

We rotate the DNA sample with planar alignment at room temperature at steps of 5° and record POM images at every step. After that, for each image, a 1  $\times$  1 mm<sup>2</sup> area is selected as the region of interest (ROI) and average intensity in the ROI is measured and normalized by

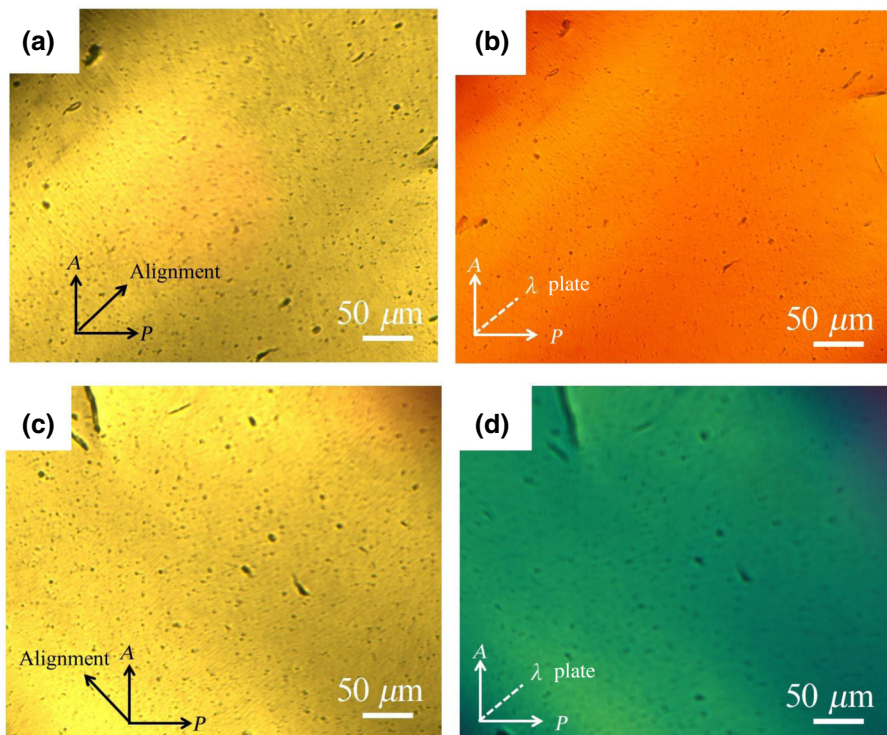
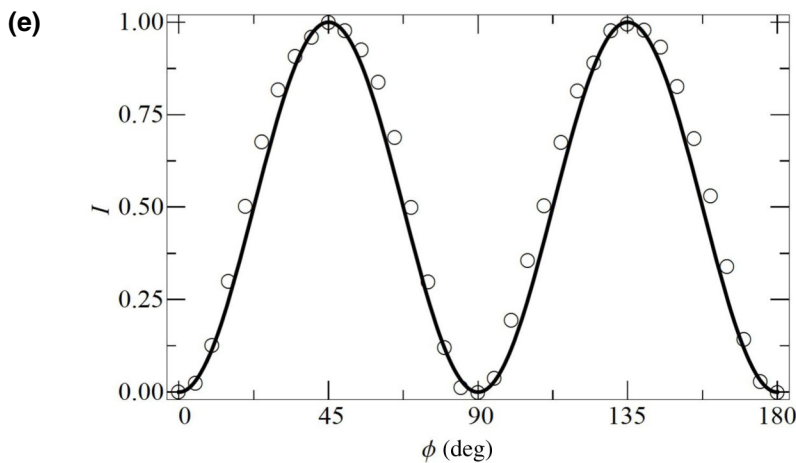


FIG. 2. Planar alignment of DNA structures by photopatterning. When aligned DNA is placed at 45° between the crossed polarizers, the texture is bright (a) and the engaged  $\lambda$ -plate POM image shows an orange color (b), which indicates that DNA structures are aligned at 45° uniformly. When aligned DNA is placed at 135° between the crossed polarizers, the texture is also bright (c) and engaged the  $\lambda$ -plate polarizing microscope image shows a light-blue color (d), which indicates that DNA molecules are aligned at 135° uniformly. (e) Transmitted intensity measurement by rotating the planar-aligned DNA sample from 0° to 180°;  $I$  is the normalized intensity and  $\phi$  is the rotation angle.



using ImageJ software. The plot of intensity at each step versus rotational angle is obtained and fitted by using  $I \propto \sin^2(2\phi)$  [43], where  $I$  is the intensity and  $\phi$  is the rotation angle, as shown in Fig. 2(e).

### C. Photopatterning DNA structures with topological defects

We first design the pattern with director field  $\hat{\mathbf{n}} = (n_x, n_y, n_z) = (\cos \theta, \sin \theta, 0)$ , where  $\theta(x, y) = m \tan^{-1}(y/x) + \theta_0$ ,  $m$  is the topological charge; the phase  $\theta_0$  sets the type of distortions. Figure 3(a) shows a pattern of director field with  $m = 1/2$  and  $\theta_0 = \pi/2$ . The director field can be simulated to gain direct visualization of the textures between cross polarizers. For every pixel, the local intensity through the crossed polarizers can be calculated

as  $I \propto \sin^2[2\theta(x, y)]$  [43]. The obtained intensity map will be normalized by dividing the intensity of every pixel by the maximum intensity of all pixels. Thus, the image graphic of the simulated texture between crossed polarizers can be plotted in Mathematica. The simulated texture between crossed polarizers is shown in Fig. 3(b). The POM image shows the texture of DNA alignment with two extinctions, Fig. 3(c), which is in agreement with the simulation. The POM image with the engaged  $\lambda$  plate is another confirmation that orientation of DNA ordering follows the predesigned pattern, Fig. 3(d). If the pattern is designed with  $m = 1$  and  $\theta_0 = \pi/2$  [Figs. 3(e) and 3(f)], the patterned DNA structures adopt bent distortions, with four extinctions imaged by POM [Fig. 3(g)], and alignment along the slow axis of the  $\lambda$  plate shows a blue color, Fig. 3(h). Pattern of DNA structures with higher

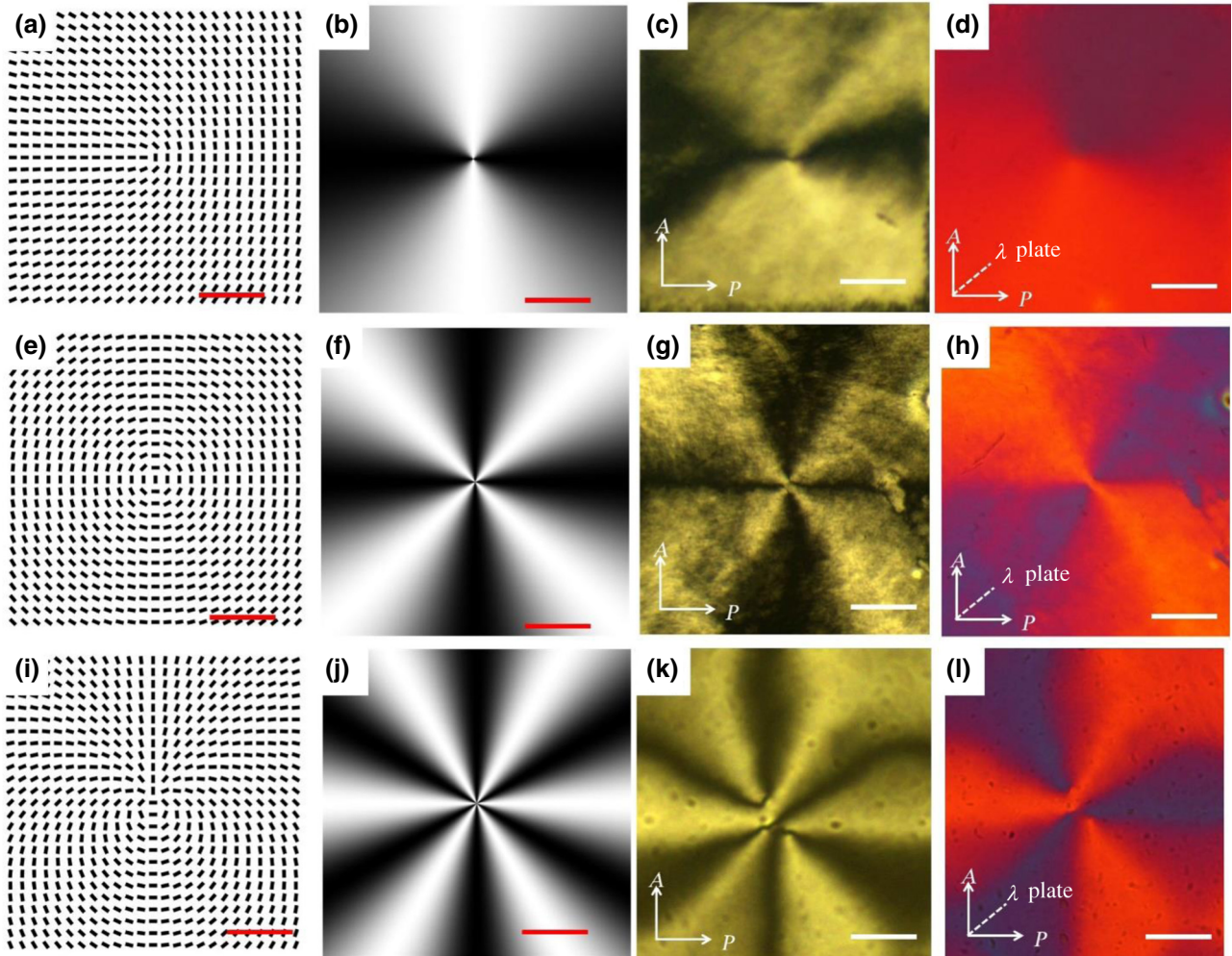


FIG. 3. Photopatterning DNA structures with topological defects. (a) Director field of a topological defect with  $m = 1/2$  and  $\theta_0 = \pi/2$ . (b) Simulated texture of 1/2 defect in part (a) between crossed polarizers. POM images of orientations of DNA structures by this 1/2 defect without (c) and with (d) the  $\lambda$  plate. (e) Director field of a topological defect with  $m = 1$  and  $\theta_0 = \pi/2$  adopting pure bent distortions. (f) Simulated texture of circular +1 defect in part (e). POM images of arrangements of DNA structures by this circular +1 defect without (g) and with (h) the  $\lambda$  plate. (i) Director field of a defect with  $m = 3/2$ . (j) Simulated texture of 3/2 defect in part (i). POM images of DNA alignment by this +3/2 defect without (k) and with (l) the  $\lambda$  plate. The scale bar is 50  $\mu\text{m}$ .

topological charge, such as  $m = 3/2$  [Figs. 3(i) and 3(j)], is also created. The POM image of this pattern shows six extinctions, Fig. 3(k), as confirmed by inserting the  $\lambda$  plate, Fig. 3(l).

#### D. Photopatterning DNA structures with 2D lattice of topological defects

To demonstrate the capability of this photopatterning technique, DNA patterns with more complex structures are created. An array of  $(+1/2, -1/2)$  defects is designed with  $\theta(x, y) = \sum_i m_i \tan^{-1}[y/(x - ix_0)]$ , where  $m_i = 1/2$ ,  $m_{i+1} = -1/2$ , and  $x_0 = 50 \mu\text{m}$  is the distance between two adjacent half defects. Then, we put these two rows of defect array with a distance  $y_0 = 100 \mu\text{m}$  to form a 2D  $(+1/2, -1/2)$  defect array, Figs. 4(a) and 4(b). DNA chains follow the predesigned pattern and POM textures are shown in Figs. 4(c) and 4(d). A 2D lattice of alternating  $(+1, -1)$  defects are created with  $\theta(x, y) = \sum_{i,j} m_{i,j} \tan^{-1}[(y - jy_0)/(x - ix_0)]$ , where  $m_{i,j} = 1$ ,  $m_{i,j+1} = -1$ , and  $x_0 = y_0 = 100 \mu\text{m}$  is the distance between the defects, Figs. 4(e) and 4(f). The POM images in Figs. 4(g) and 4(h) show the alignment of DNA structures by the pre-designed pattern in Fig. 4(f). A more complex pattern of DNA ordering with a 2D lattice of  $(+3/2, -3/2)$  defects are shown in Figs. 4(i)–4(l).

and 4(h) show the alignment of DNA structures by the pre-designed pattern in Fig. 4(f). A more complex pattern of DNA ordering with a 2D lattice of  $(+3/2, -3/2)$  defects are shown in Figs. 4(i)–4(l).

#### E. Photopatterning DNA structures with scale-up arbitrary geometries

Scaled-up arbitrary shapes of DNA structures can be created by programming the patterns. For example, letters of “U” and “M” with alignment along  $135^\circ$  are designed, Fig. 5(a), and the patterns of DNA structures are imaged by POM in Figs. 5(b) and 5(c). The domains with “UM” align DNA chains along  $135^\circ$ , showing a bright texture, Fig. 5(b), and the alignment of DNA structures is confirmed with insertion of the  $\lambda$  plate, Fig. 5(c). Other scaled-up arbitrary patterns, such as *Mona Lisa* and *The Starry Night* paintings, are also created, Figs. 5(d)–5(g). Figure 5(d) shows the mask of the *Mona Lisa* painting, with white pixels transmitting light with linear polarization along  $45^\circ$  and black pixels blocking light. The POM image shows that DNA chains are patterned following the

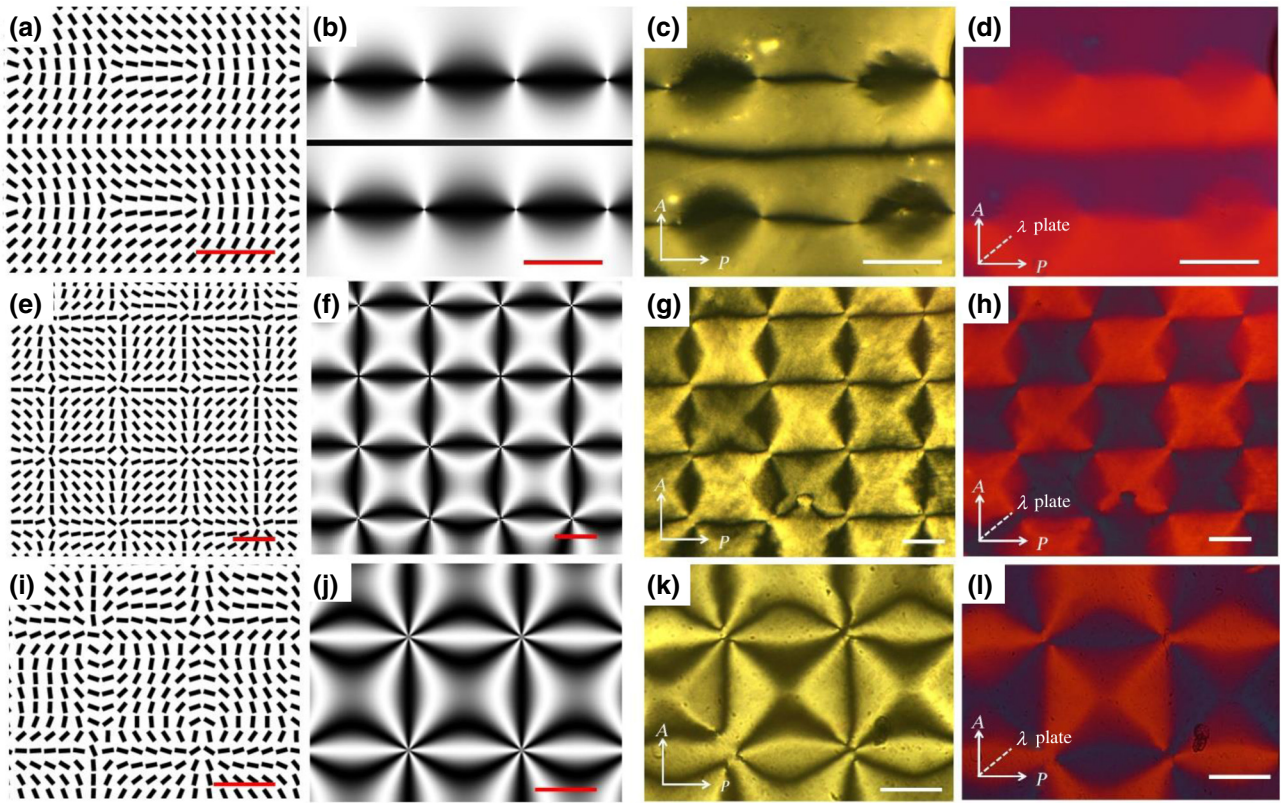


FIG. 4. Photopatterning DNA structures with 2D array of topological defects. (a) Director field of a 2D lattice of defects  $(+1/2, -1/2)$ . (b) Simulated texture of director field in part (a) between crossed polarizers. POM images of DNA alignment by the pattern without (c) and with (d) the  $\lambda$  plate. (e) Director field of a 2D defect array of  $(+1, -1)$ . (f) Simulated texture of director field in part (e). POM images of DNA pattern by the  $(+1, -1)$  defect array without (g) and with (h)  $\lambda$  plate. (i) Director field of a 2D defect array of  $(+3/2, -3/2)$ . (j) Simulated texture of director field in part (i). POM images of DNA alignment by the  $(+3/2, -3/2)$  defect array without (k) and with (l) the  $\lambda$  plate. The scale bar is  $50 \mu\text{m}$ .

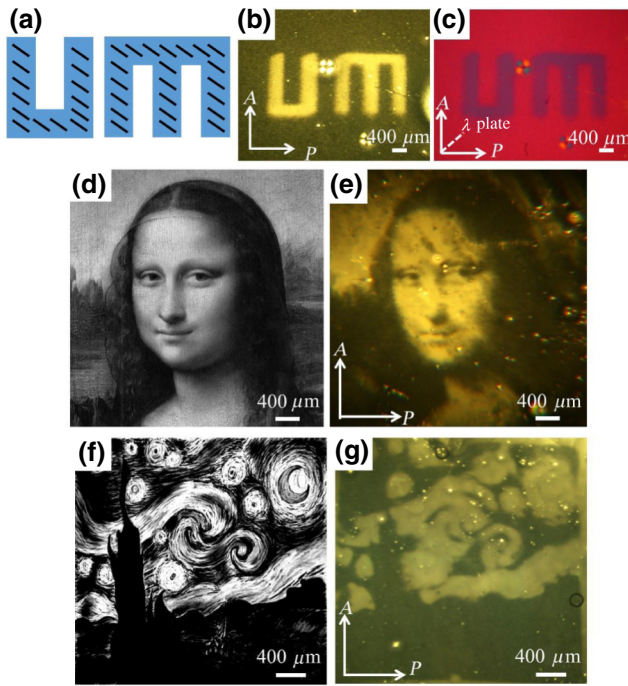


FIG. 5. Arbitrary shapes of scaled-up patterns of DNA structures. (a) Designed alignment at  $135^\circ$  with respect to the horizontal direction. POM images of patterns of DNA chains in the form of letters “U” and “M” without (b) and with (c) the  $\lambda$  plate. (d) Mask with the pattern of the *Mona Lisa* painting, with white pixels transmitting linearly polarized light along  $45^\circ$  and black pixels blocking light. (e) POM image of the pattern with bright pixels indicating DNA chains are aligned at  $45^\circ$ , following the design. Mask with the pattern of van Gogh’s *The Starry Night* painting (f) and POM image of the pattern, with bright pixels indicating that DNA chains are aligned along the  $45^\circ$  direction (g).

design, with bright domains aligned at  $45^\circ$  with respect to the polarizer, Fig. 5(e). The mask with the pattern of van Gogh’s *The Starry Night* painting and a POM image of the pattern of DNA chains are shown in Figs. 5(f) and 5(g), respectively. Notably, the patterns in these experiments are scaled up to the range of several millimeters. For Figs. 5(e) and 5(g), a higher magnification lens is used to obtain larger scale patterns, which will cause more image aberration during patterning and the resolution will be compromised.

### III. CONCLUSION

Here, we demonstrate how to use the anisotropies in liquid-crystal polymers to control the complex macroscopic patterns of DNA structures emerging from simple interacting microscopic constituents. Although the molecular mechanism of how the DNA molecule interacts with the liquid-crystal polymer requires further exploration, this work expands the potential utility of liquid-crystal

polymers into the realm of DNA lyotropic systems. It will shed light on future research directions, such as the study of the viscoelastic properties of this system by using the alignment method demonstrated in this work, the exploration of molecular structures in the defect core produced by this work, and theoretical modeling of DNA molecular self-assemblies and their interactions with liquid-crystal polymers, etc.

Additionally, the aligned DNA chains are widely used as a template for the self-assembly of bacteria [42], gold nanorods [23,44], thermotropic liquid-crystal molecules [16], etc. As a type of aqueous lyotropic liquid crystal, the ordered DNA structures shown here can potentially be designed to direct the assembly of peptide amphiphiles [45,46] and other kinds of biomolecules [47,48]. As shown in Fig. 1, the concentration of DNA we use has an isotropic phase at a temperature of  $95^\circ\text{C}$ . At temperatures higher than this temperature, the DNA molecules are oriented randomly, but at lower temperatures, such as room temperature, the molecules recover the designed ordered structures. If DNA is used as a template material, this property will help to realize the reconfiguration of suspended biomaterials by simply changing the temperature. Due to the simplicity and versatility of our technique in this work, this programmable and biocompatible soft material, across multiple length scales, will find applications as templating tools for various guest functional materials to follow the orientations of ordered DNA chains.

To summarize, space-varying DNA self-assembled structures, in a deterministically predesigned manner, can be created by using the photopatterning technique. Various configurations of DNA orientations with a 2D lattice of topological defects are achieved by placing DNA molecules inside a cell coated with photopatterned liquid-crystalline polymer. Additionally, this method can be fine-tuned to scale up and arbitrary patterns of DNA chains in the millimeter-scale range are created. The arbitrary patterns of DNA structures are not limited to the current work and can be programmed to different geometries due to the versatility of the designed patterns. The resulting programmable and predesigned DNA self-assembled structures across multiple length scales will open up opportunities for designing dynamic functional bionanomaterials and developing electro-optical and biosensing devices.

### ACKNOWLEDGMENTS

This work is supported by University of Memphis startup funds. The authors thank Dr. Oleg Lavrentovich and Dr. Qi-Huo Wei for fruitful discussions.

N.P.D. and J.J. contributed equally to this work. N.P.D. and J.J. performed the experiments. Y.G. fabricated the metmask. C.P. conceived and directed the research. All authors analyzed the data and participated in discussing and writing the manuscript.

- [1] G. M. Whitesides and B. Grzybowski, Self-assembly at all scales, *Science* **295**, 2418 (2002).
- [2] J. D. Watson and F. H. Crick, “The structure of DNA”, presented at *Cold Spring Harbor Symposia on Quantitative Biology* (1953).
- [3] E. Winfree, F. Liu, L. A. Wenzler, and N. C. Seeman, Design and self-assembly of two-dimensional DNA crystals, *Nature* **394**, 539 (1998).
- [4] P. W. K. Rothemund, Folding DNA to create nanoscale shapes and patterns, *Nature* **440**, 297 (2006).
- [5] E. S. Andersen, M. Dong, M. M. Nielsen, K. Jahn, R. Subramani, W. Mamdouh, M. M. Golas, B. Sander, H. Stark, C. L. P. Oliveira, J. S. Pedersen, V. Birkedal, F. Besenbacher, K. V. Gothelf, and J. Kjems, Self-assembly of a nanoscale DNA box with a controllable lid, *Nature* **459**, 73 (2009).
- [6] H. Dietz, S. M. Douglas, and W. M. Shih, Folding DNA into twisted and curved nanoscale shapes, *Science* **325**, 725 (2009).
- [7] G. Tikhomirov, P. Petersen, and L. Qian, Fractal assembly of micrometre-scale DNA origami arrays with arbitrary patterns, *Nature* **552**, 67 (2017).
- [8] A. Sassolas, B. D. Leca-Bouvier, and L. J. Blum, DNA biosensors and microarrays, *Chem. Rev.* **108**, 109 (2008).
- [9] H. Qi, G. Huang, Y. Han, X. Zhang, Y. Li, B. Pingguan-Murphy, T. J. Lu, F. Xu, and L. Wang, Engineering artificial machines from designable DNA materials for biomedical applications, *Tissue Eng. Part B Rev.* **21**, 288 (2014).
- [10] D. Woods, D. Doty, C. Myhrvold, J. Hui, F. Zhou, P. Yin, and E. Winfree, Diverse and robust molecular algorithms using reprogrammable DNA self-assembly, *Nature* **567**, 366 (2019).
- [11] T. Li, L. Zhang, J. Ai, S. Dong, and E. Wang, Ion-tuned DNA/Ag fluorescent nanoclusters as versatile logic device, *ACS Nano* **5**, 6334 (2011).
- [12] M. Hamed, A. Elfwing, R. Gabrielsson, and O. Inganäs, Electronic polymers and DNA self-assembled in nanowire transistors, *Small* **9**, 363 (2013).
- [13] I. I. Smalyukh, O. V. Zribi, J. C. Butler, O. D. Lavrentovich, and G. C. L. Wong, Structure and Dynamics of Liquid Crystalline Pattern Formation in Drying Droplets of DNA, *Phys. Rev. Lett.* **96**, 177801 (2006).
- [14] B. Li, W. Han, M. Byun, L. Zhu, Q. Zou, and Z. Lin, Macroscopic highly aligned DNA nanowires created by controlled evaporative self-assembly, *ACS Nano* **7**, 4326 (2013).
- [15] N. Morii, G. Kido, H. Suzuki, S. Nimori, and H. Morii, Molecular chain orientation of DNA films induced by both the magnetic field and the interfacial effect, *Biomacromolecules* **5**, 2297 (2004).
- [16] Y. J. Cha and D. K. Yoon, Control of periodic zigzag structures of DNA by a simple shearing method, *Adv. Mater.* **29**, 1604247 (2017).
- [17] A. Bensimon, A. Simon, A. Chiffaudel, V. Croquette, F. Heslot, and D. Bensimon, Alignment and sensitive detection of DNA by a moving interface, *Science* **265**, 2096 (1994).
- [18] T. Perkins, D. Smith, R. Larson, and S. Chu, Stretching of a single tethered polymer in a uniform flow, *Science* **268**, 83 (1995).
- [19] X. Michalet, R. Ekong, F. Fougerousse, S. Rousseaux, C. Schurra, N. Hornigold, M. v. Slegtenhorst, J. Wolfe, S. Povey, J. S. Beckmann, and A. Bensimon, Dynamic molecular combing: Stretching the whole human genome for high-resolution studies, *Science* **277**, 1518 (1997).
- [20] J. Guan and L. J. Lee, Generating highly ordered DNA nanostrand arrays, *Proc. Natl. Acad. Sci. U. S. A.* **102**, 18321 (2005).
- [21] D. K. Yoon, G. P. Smith, E. Tsai, M. Moran, D. M. Walba, T. Bellini, I. I. Smalyukh, and N. A. Clark, Alignment of the columnar liquid crystal phase of nano-DNA by confinement in channels, *Liq. Cryst.* **39**, 571 (2012).
- [22] S. Nagashima, H. D. Ha, D. H. Kim, A. Košmrlj, H. A. Stone, and M.-W. Moon, Spontaneous formation of aligned DNA nanowires by capillarity-induced skin folding, *Proc. Natl. Acad. Sci. U. S. A.* **114**, 6233 (2017).
- [23] Y. J. Cha, S. M. Park, R. You, H. Kim, and D. K. Yoon, Microstructure arrays of DNA using topographic control, *Nat. Commun.* **10**, 2512 (2019).
- [24] T. E. Strzelecka, M. W. Davidson, and R. L. Rill, Multiple liquid crystal phases of DNA at high concentrations, *Nature* **331**, 457 (1988).
- [25] F. Livolant, A. M. Levelut, J. Doucet, and J. P. Benoit, The highly concentrated liquid-crystalline phase of DNA is columnar hexagonal, *Nature* **339**, 724 (1989).
- [26] Y. Guo, M. Jiang, C. Peng, K. Sun, O. Yaroshchuk, O. D. Lavrentovich, and Q.-H. Wei, High-resolution and high-throughput plasmonic photopatterning of complex molecular orientations in liquid crystals, *Adv. Mater.* **28**, 2353 (2016).
- [27] C. Peng, T. Turiv, Y. Guo, S. V. Shiyanovskii, Q.-H. Wei, and O. D. Lavrentovich, Control of colloidal placement by modulated molecular orientation in nematic cells, *Sci. Adv.* **2**, e1600932 (2016).
- [28] C. Peng, Y. Guo, T. Turiv, M. Jiang, Q.-H. Wei, and O. D. Lavrentovich, Patterning of lyotropic chromonic liquid crystals by photoalignment with photonic metamasks, *Adv. Mater.* **29**, 1606112 (2017).
- [29] C. Peng, T. Turiv, Y. Guo, Q.-H. Wei, and O. D. Lavrentovich, Command of active matter by topological defects and patterns, *Science* **354**, 882 (2016).
- [30] R. Ros, R. Eckel, F. Bartels, A. Sischka, B. Baumgarth, S. D. Wilking, A. Pühler, N. Sewald, A. Becker, and D. Anselmetti, Single molecule force spectroscopy on ligand–DNA complexes: From molecular binding mechanisms to biosensor applications, *J. Biotechnol.* **112**, 5 (2004).
- [31] N. Sewald, S. D. Wilking, R. Eckel, S. Albu, K. Wollschläger, K. Gaus, A. Becker, F. W. Bartels, R. Ros, and D. Anselmetti, Probing DNA–peptide interaction forces at the single-molecule level, *J. Pept. Sci.* **12**, 836 (2006).
- [32] H. Nakao, H. Shiigi, Y. Yamamoto, S. Tokonami, T. Nagaoka, S. Sugiyama, and T. Ohtani, Highly ordered assemblies of Au nanoparticles organized on DNA, *Nano Lett.* **3**, 1391 (2003).
- [33] M. G. Warner and J. E. Hutchison, Linear assemblies of nanoparticles electrostatically organized on DNA scaffolds, *Nat. Mater.* **2**, 272 (2003).
- [34] A. Kumar, M. Pattarkine, M. Bhadbhade, A. B. Mandale, K. N. Ganesh, S. S. Datar, C. V. Dharmadhikari, and M.

- Sastray, Linear superclusters of colloidal gold particles by electrostatic assembly on DNA templates, *Adv. Mater.* **13**, 341 (2001).
- [35] C. Peng, Y. Guo, C. Conklin, J. Viñals, S. V. Shiyanovskii, Q.-H. Wei, and O. D. Lavrentovich, Liquid crystals with patterned molecular orientation as an electrolytic active medium, *Phys. Rev. E* **92**, 052502 (2015).
- [36] C. Peng, T. Turiv, Y. Guo, Q.-H. Wei, and O. D. Lavrentovich, Sorting and separation of microparticles by surface properties using liquid crystal-enabled electro-osmosis, *Liq. Cryst.* **45**, 1936 (2018).
- [37] C. Peng and O. Lavrentovich, Liquid crystals-enabled AC electrokinetics, *Micromachines* **10**, 45 (2019).
- [38] C. Peng, T. Turiv, R. Zhang, Y. Guo, S. V. Shiyanovskii, Q.-H. Wei, J. de Pablo, and O. D. Lavrentovich, Controlling placement of nonspherical (boomerang) colloids in nematic cells with photopatterned director, *J. Phys.: Condens. Matter* **29**, 014005 (2017).
- [39] Y. Guo, M. Jiang, C. Peng, K. Sun, O. Yaroshchuk, O. D. Lavrentovich, and Q.-H. Wei, Designs of plasmonic metamasks for photopatterning molecular orientations in liquid crystals, *Crystals* **7**, 8 (2017).
- [40] K. Tanaka and Y. Okahata, A DNA–lipid complex in organic media and formation of an aligned cast film1, *J. Am. Chem. Soc.* **118**, 10679 (1996).
- [41] M. Nakata, G. Zanchetta, B. D. Chapman, C. D. Jones, J. O. Cross, R. Pindak, T. Bellini, and N. A. Clark, End-to-end stacking and liquid crystal condensation of 6– to 20–base pair DNA duplexes, *Science* **318**, 1276 (2007).
- [42] I. I. Smalyukh, J. Butler, J. D. Shroud, M. R. Parsek, and G. C. L. Wong, Elasticity-mediated nematiclike bacterial organization in model extracellular DNA matrix, *Phys. Rev. E* **78**, 030701 (2008).
- [43] A. Jákli and A. Saupe, *One-and two-Dimensional Fluids: Properties of Smectic, Lamellar and Columnar Liquid Crystals* (CRC Press, Florida, U.S.A., 2006).
- [44] Y. J. Cha, D. S. Kim, and D. K. Yoon, Highly aligned plasmonic gold nanorods in a DNA matrix, *Adv. Funct. Mater.* **27**, 1703790 (2017).
- [45] P. van der Asdonk, M. Keshavarz, P. C. M. Christianen, and P. H. J. Kouwer, Directed peptide amphiphile assembly using aqueous liquid crystal templates in magnetic fields, *Soft Matter* **12**, 6518 (2016).
- [46] P. van der Asdonk, H. C. Hendrikse, M. Fernandez-Castano Romera, D. Voerman, B. E. I. Ramakers, D. W. P. M. Löwik, R. P. Sijbesma, and P. H. J. Kouwer, Patterning of soft matter across multiple length scales, *Adv. Funct. Mater.* **26**, 2609 (2016).
- [47] P. van der Asdonk and P. H. J. Kouwer, Liquid crystal templating as an approach to spatially and temporally organise soft matter, *Chem. Soc. Rev.* **46**, 5935 (2017).
- [48] M. Rodriguez Sala, C. Peng, O. Skalli, and F. Sabri, Tunable neuronal scaffold biomaterials through plasmonic photo-patterning of aerogels, *MRS Commun.* **9**, 1249 (2019).